Roles of apoptosis and autophagy in natural rabies infections

Mustafa Ozkaraca[1]*, Selcuk Ozdemir[2], Selim Comakli[3],
Mehmet Ozkan Timurkan[4]

[1]Department of Pathology, Faculty of Veterinary Medicine, Cumhuriyet University, Sivas, Turkey
[2]Department of Genetic, Faculty of Veterinary Medicine, Ataturk University, Erzurum, Turkey
[3]Department of Pathology, Faculty of Veterinary Medicine, Ataturk University, Erzurum, Turkey
[4]Department of Virology, Faculty of Veterinary Medicine, Ataturk University, Erzurum, Turkey

*Corresponding author: mustafaozkaraca@cumhuriyet.edu.tr

Abstract: The aim of this study was to investigate the activity of apoptosis and autophagy in animals (cows, horses, donkeys, dogs and cats) naturally infected with rabies by using immunohistochemistry, immunofluorescence, and qPCR. The mRNA transcript levels of *caspase-3*, *Bax*, *Bcl2* and *LC3B* were determined with qPCR. Caspase-3 and AIF immunopositivity were not observed in the immunohistochemical and immunofluorescence staining, whereas LC3B immunopositivity was determined intensively in the infected animals compared to the control groups. LC3B immunopositivity was detected in the cytoplasm of the Purkinje cells in the cerebellum of the cows, horses and donkeys, and also in the cytoplasm of the neurons in the cornu ammonis of the dogs and cats. While the expression levels of caspase-3 and Bax were downregulated, the Bcl2 expression was up-regulated in the infected animals compared to the uninfected animals. In addition, the LC3B levels were found to be significantly higher in the infected animals. To the best of our knowledge, this work represents the first report of neuronal death in the central nervous system by autophagy, rather than by caspase-dependent or AIF-containing caspase-independent apoptosis.

Keywords: AIF; caspase-3; LC3B

Rabies is a disease that causes acute encephalitis in the central nervous system and the subsequent death in humans and animals. The rabies virus belongs to the genus *Lyssavirus* of the *Rhabdoviridae* family (Jackson 2003). The disease is spread by intramuscular or subcutaneous transport of an infected mammal's saliva (Warrell and Warrell 2004). Previous studies have reported that changes in rabies-infected neurons are not fully understood and this remains the case (Jackson 1993; Dumrongphol et al. 1996; Jackson 2011; Kip et al. 2017). Nevertheless, models of cell death involving apoptosis and autophagy have been studied *in vivo* and *in vitro* (Jackson and Park 1998; Yan et al. 2001; Sarmento et al. 2005; Sarmento et al. 2006; Scott et al. 2008; Suja et al. 2011; Peng et al. 2016; Zan et al. 2016; Li et al. 2017; Liu et al. 2017).

Caspases have an important role in apoptosis (Sarmento et al. 2006). There are two pathways involved in apoptosis caused by caspases. The first is an extrinsic pathway initiated by the cell surface receptors with activation of caspase-8. The second is an intrinsic pathway organised by the mitochondria and with activation of caspase-9. Caspase-3 is active in both pathways (Ashkenazi and Dixit 1998; Budihardjo et al. 1999; Granville and Gottlieb 2002). In addition, a flavoprotein caspase [i.e., apoptosis-inducing factor (AIF)] is released from the mitochondria and initiates an independent pathway (Susin et al. 1999; Galluzzi et al. 2012). The AIF release from the mitochondria to the cytoplasm is a critical initiative stage in the mitochondrial apoptotic process (Huang et al. 2016). AIF signalling pathway-mediated apoptosis is one

of the non-caspase-dependent cell death mechanisms that are widely present in neurological diseases (Nan et al. 2020). The members of the BCL2 family are key regulators of apoptosis (Adams and Cory 1998). Based on their function, BCL2 family members are classified in one of two groups: proapoptotic vs antiapoptotic proteins. The proapoptotic BCL2 family proteins, such as BAX, BAD, BID and BCLXS, trigger and/or promote apoptosis, whereas the antiapoptotic members of this family, including BCL2, BCLXL and BCLW, protect the cell by impeding the normal cell death (Youle and Strasser 2008). Interestingly, the relative expression ratios of the pro- and antiapoptotic BCL2-family members dictate the cell fate and sensitivity (or resistance) of cells to multiple apoptotic stimuli, including infections, growth factor deprivation, hypoxia, exposure to oxidants, irradiation, and treatment with antineoplastic agents (Shinoura et al. 1999; Giotakis et al. 2016).

Autophagic cell death, which is a more recent issue, has been reported to be an important pathway for the removal of intracellular pathogens from the cell such as viruses (Liu et al. 2017). In addition, microtubule-associated protein 1 light chain 3 (LC3) is an important marker controlled by autophagy-related (ATG) genes during autophagy (Kirkegaard et al. 2004; Warrell and Warrell 2004; Yang et al. 2005; Klionsky et al. 2012). In previous *in vivo* and *in vitro* studies, the rabies virus has been reported to cause apoptosis (Yan et al. 2001; Thoulouze et al. 2003; Sarmento et al. 2005; Sarmento et al. 2006; Zan et al. 2016). Recent studies have shown that the virus causes autophagy *in vitro* (Peng et al. 2016; Li et al. 2017; Liu et al. 2017). However, there is no detailed data on apoptosis and autophagy mechanism in animals infected with a natural rabies virus.

This study aimed to evaluate the apoptosis and autophagy in animals (cows, horses, donkeys, dogs and cats) naturally infected with rabies by using different methods such as immunohistochemistry, immunofluorescence and quantitative polymerase chain reaction (qPCR).

MATERIAL AND METHODS

Animals

The brain samples (*n* = 3 for each species) were taken from five different species (cows, horses,

donkeys, dogs, and cats) that had been diagnosed with natural rabies by qPCR.

In addition, brain samples (*n* = 3 for each species) of cows, horses, donkeys, dogs and cats without rabies were used as negative controls. Five animals were selected from each of the species included in the study. The cerebellum in the herbivores (cows, horses, and donkeys) and the cornu ammonis region in the carnivores (dogs and cats) were examined by immunohistochemistry, immunofluorescence, and qPCR.

Immunohistochemistry detection of caspase-3, AIF and LC3B

The cerebellum and cornu ammonis tissues were fixed in 10% neutral buffered formalin, embedded in paraffin after dehydration in graded ethanol, clearing in xylene. Tissues were cut into 5 μm and placed onto poly-L-lysine coated slides. The sections were then deparaffinised, rehydrated, and placed in 3% hydrogen peroxide to block the endogenous peroxidase activity. The sections were pre-treated in a citrate buffer (pH 6.0) in a microwave for 15 minutes.

Then, sections were incubated with primary antibodies for caspase-3 antibodies (Novus Biological, Littleton, CO, USA; Cat. No. NB600-1235, dilution 1 : 400), AIFM1 antibodies (Aviva System Biology, San Diego, CA, USA; Cat. No. AVARP02013_P050, dilution 1 : 400) and anti-LC3B antibodies (Abcam, Cambridge, UK; Cat. No. ab48394, dilution 1 : 400) at 37 °C for 1 hour.

After a phosphate buffer solution (PBS) wash, the sections were incubated with the secondary antibodies [EXPOSE Mouse and Rabbit Specific HRP/DAB detection IHC kit (Abcam; Cambridge, UK; Cat. No. ab80436)] at room temperature for 20 minutes. The tissue sections were analysed using 3,3'-diaminobenzidine (DAB) chromogen for colorimetric visualisation. The sections were counter-stained with Mayer's haematoxylin. The immunopositivity was evaluated as negative (−) or positive (+).

Immunofluorescence detection of caspase-3, AIF and LC3B

After deparaffinisation, the slides were boiled in an antigen retrieval solution (pH 6.0) (Cat. No. ab96674; Abcam, Cambridge, UK) in a microwave

for 15 min to unmask the antigens. The sections were incubated for 15 min with a protein block solution (Abcam, Cambridge, UK; Cat. No. ab80436;) to prevent nonspecific binding. The sections were incubated at 37 °C with caspase-3 antibodies (Novus Biological, Littleton, CO, USA; Cat. No. NB600-1235, dilution 1 : 400), AIFM1 antibodies (Aviva System Biology, San Diego, CA, USA; Cat. No. AVARP02013_P050, dilution 1 : 400) and anti-LC3B antibodies (Abcam, Cambridge, UK; Cat. No. ab48394, dilution 1 : 400) for 45 minutes. The sections were washed with PBS for 5 minutes. After washing, Goat Anti-Rabbit IgG H&L (FITC) (Abcam, Cambridge, UK; Cat. No. ab6717, dilution 1 : 50) was used as a secondary antibody at 37 °C for 30 minutes. Finally, all the sections were covered with a Fluoroshield Mounting Medium with DAPI (Abcam, Cambridge, UK; Cat. No. ab104140) for evaluation by fluorescence microscopy (Zeiss Scope A1 with an Axio cam ICc5 camera attachment system; Zeiss, Oberkochen, Germany). The immunopositivity was evaluated as being either negative (–) or positive (+).

Total RNA isolation

Three formalin-fixed, paraffin-embedded (FFPE) brain sections were subjected to deparaffinisation in accordance with the methodology of a previous study (Vahed et al. 2016). The total RNA isolation was achieved from the collected FFPE biopsy samples through the utilisation of Trizol (Invitrogen, Carlsbad, CA, USA). The total RNA isolation was achieved according to kit manufacturer's instructions. Following the total RNA isolation, the RNA concentration was measured using NanoDrop (Epoch Microplate Spectrophotometer; BioTek Instruments, Inc, Winooski, VT, USA). The RNA samples were set in 1.5% agarose gel in a 1XTBE solution for 1 h at 80 V (volts) with the goal of controlling the total RNA quality and was visualised by a gel imaging system (Bio-Rad Gel Doc XR+; Hercules, CA, USA). The RNA quality was then determined.

DNase I treatment and cDNA synthesis

DNase I (Thermo Scientific, Waltham, MA, USA) was used to prevent any DNA contamination in the isolated RNA samples. The DNase I treatment was performed in line with the protocol provided in the kit. Subsequently, 1 μg was taken from these RNAs and the cDNA was synthesised through utilisation of a miScript Reverse Transcription Kit (Qiagen, Hilden, Germany) in accordance with the protocol provided. The purity and quantity of the obtained cDNAs were measured with a spectrophotometer (Epoch Microplate Spectrophotometer; BioTek Instruments, Winooski, VT, USA) and the cDNAs were diluted at the same ratios. The cDNA samples were then stored at −20 °C for utilisation in real-time polymerase chain reaction (PCR) studies (Comakli et al. 2020).

qPCR

The primers used for the diagnosis of the rabies virus were identified by Nagaraj et al. (2006). SYBR Green was used in the qPCR and a melting curve was added after the study to prevent possible false reactions.

The qPCR was performed through utilisation of a CFX96 BioRad device in order to measure the mRNA transcript levels of the *caspase-3*, *Bax*, *Bcl2*, and *LC3B* genes. The *beta-actin* gene was employed as an internal control. The master mix content created in the real-time PCR experiments included a SYBR Green 2X Rox Dye Master Mix (Qiagen, Hilden, Germany), forward and reverse primers designed for genes, cDNAs as templates and nuclease-free water. The samples were analysed in a qPCR device following the preparation of the master mixes and the obtained Ct values were calculated according to the $2^{-\Delta\Delta Ct}$ method.

The expression levels of the respective genes were determined (Livak and Schmittgen 2001). The primer sequences of the genes are shown in Tables 1 and 2.

Statistical analysis

The IBM SPSS v20 (IBM, USA) program was employed for the statistical analysis. The statistical differences of the mRNA transcript levels of the *caspase-3*, *Bax*, *Bcl2*, and *LC3B* genes were analysed by a one-way analysis of variance (ANOVA). For statistical comparisons, probability levels of $P < 0.05$, $P < 0.01$, and $P < 0.001$ were accepted as statistically significant.

Table 1. Primer sequences of *caspase-3*, *Bax*, *Bcl2*, *LC3B*, and *beta-actin*

Gene	Horse	Donkey	Cow	Cat	Dog
Caspase-3	F: ATTATTCAGGCCTGCC-GAGG	F: ATTATTCAGGCCTGCC-GAGG	F: CAGGCGTCGTAGCTGAAC-GTA	F: CAAATTGTGGCGTTGC TGGA	F: CGGGAATGTCCTTGA-CAAC
	R: GCGATGAAAGCGGCA TGTTT	R: GCGATGAAAGCGGCA TGTTT	R: CGACAGGCCATGCCAG-TATT	R: CCTCGGCAGGCCTGAA TAAT	R: TGTTTCCCTGAGGTTT-GCTG
Bax	F: CCTCTCCGACTTTGGG TCAC	F: CCTCTCCGACTTTTGG GTCAC	F: TGAAGGCGCATCGGAGAT GAAT	F: AATTGCAGAGGATGAT CGCAGC	F: GAGTTGCAGAGGATGA TCGCAG
	R: CAAGGAGGTTTATTGC CCCC	R: AAGAGTCACAGTCCA AGGCAG	R: CCTTGAGCACCAGTTT-GCTG	R: GCAAAGTAGAAGAGG GCAACG	R: TGAGTGACGCAGTAAG CACT
Bcl2	F: GGAGAACAGGGTATGA TAAC	F: GCGCACGCTGGGAG AACAGG	F: AGGCTACGATAACCGAG AGA	F: TGCCACGGTGGTGGAG-GAGC	F: CGCTGGGCGGCAACAGGG-TACG
	R: CAAAGAAGGCCACAA TCCTC	R: TCCCCTCGCGGTGAA AGGCG	R: CAGTGCCTTCAGAGAC AGCC	R: TGGCCCAGATAGGCA CCCAGGGTG	R: AGCGTCCCCTCGCGGT-GAAG
LC3B	F: TGAGGAGACACAAGG GAAGTC	F: ACAGGTGGTAAGAGT CCTTGG	F: GTCCGACTTATCCGAG AGCA	F: AGATCATTAGGAGGCG CTTACA	F: GTCGCACCTTCGAACA AAGA
	R: GAGCTGTAAGCGCCT TCTAAT	R: TGCTGCTCTCGGATA-AGTCG	R: TGAGCTGTAAGCGCCT TCTT	R: GGAGCTCCATTTTTCT-GCTTGTAG	R: AGCTGTAAGCGCCTCC TAAT
Beta-actin	F: AGTGTGACGTCGACA TCCGT	F: CTGAGCGCAAGTACT CCGTA	F: GTCGACACCGCAACCA GTTC	F: AGCCATTTTCTGTTCC-GCCT	F: GTCACCAACTGGGACG ACAT
	R: AGCCGCCGATCCAT ACG	R: CTAACAGTCCGCCTA GAAGCA	R: TACGAGTCCTTCTGGC CCAT	R: GGCATGCCACAAATGT-GATGT	R: CATCTTCTCACGGTTG-GCCT

Table 2. Primer sequences of the size base pairs and accession number

Gene	Horse	Donkey	Cow	Cat	Dog
Caspase-3	495 bp, XM_023630401.1	206 bp, XM_014839504.1	225 bp, NM_001077840.1	212 bp, NM_001009338.1	146 bp, NM_001003042.1
Bax	238 bp, XM_023650077.1	127 bp, XM_014852261.1	183 bp, NM_173894.1	127 bp, DQ926869.1	334 bp, NM_001003011.1
Bcl2	321 bp, XM_001490436.4	335 bp, XM_014843803.1	400 bp, NM_001166486.1	314 bp, DQ926871.1	320 bp, NM_001002949.1
LC3B	321 bp, XM_023637465.1	420 bp, XM_014835085.1	163 bp, NM_001001169.1	361 bp, XM_023245115.1	190 bp, XM_536756.5
Beta-actin	160 bp, NM_001081838.1	143 bp, XM_014835097.1	181 bp, AY141970.1	169 bp, GQ848333.1	181 bp, AY141970.1

RESULTS

Detection of rabies in brain tissues

The mean cycle threshold (Ct) values and melting curve temperatures obtained after the real-time PCRs in five different animal species with rabies infection are shown in Table 3. According to the

Table 3. The detection of rabies with RT-PCR in the infected animals

RT-PCR	Horse	Donkey	Cow	Cat	Dog
Mean cycle threshold	30.38	29.96	29.84	29.94	29.72
Melting curve (°C)	82.0	82.0	82.0	82.0	82.0
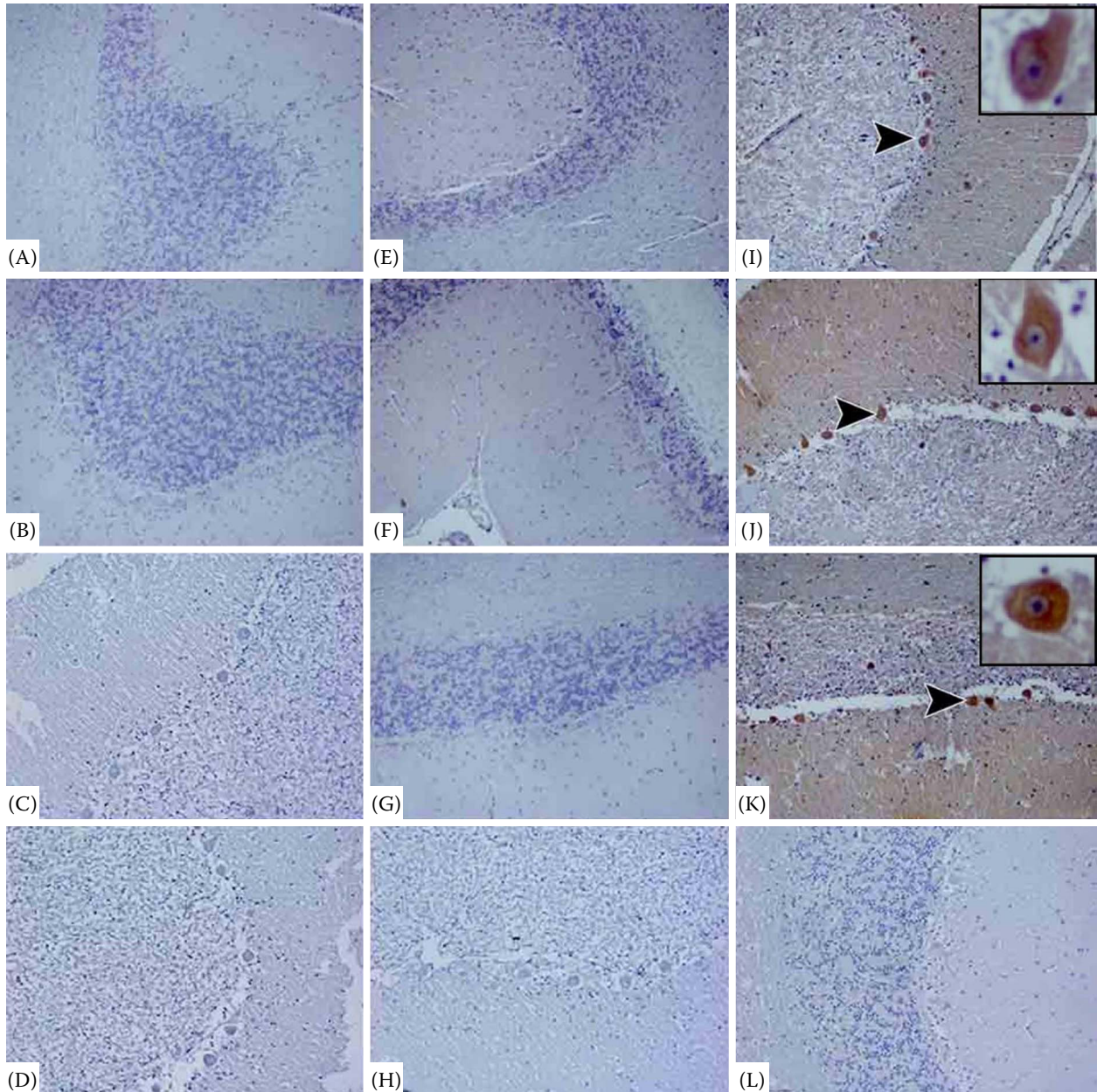
Figure 1. Cerebellum. Natural rabies infection activated LC3B, but not caspase-3 and AIF

Cerebellum sections showing negative staining for caspase-3 in the granule cells and Purkinje cell compartments of the rabies-infected cow (A), horse (B), donkey (C), and control (D) animals. View of negative staining for AIF in the granule cells and Purkinje cell compartments of the cerebellum of the rabies-infected cow (E), horse (F), donkey (G), and control (H) animals. Purkinje cell compartments of cerebellum showing strong positive signals for LC3B in the rabies-infected cow (I), horse (J), donkey (K), but not LC3B positivity in the control animals (L). IHC × 20
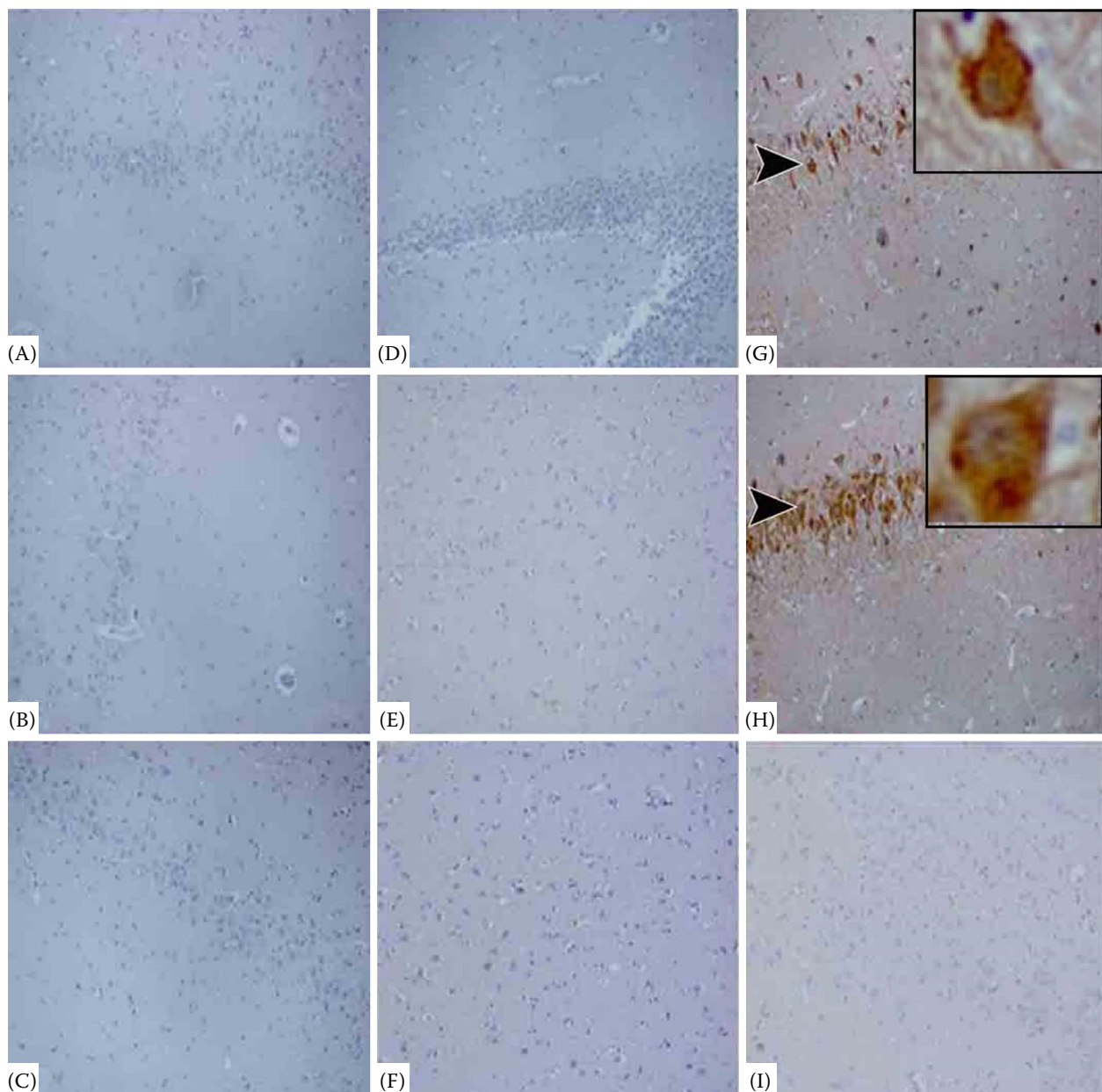
Figure 2. Cornu ammonis. Natural rabies infection activated LC3B, but not caspase-3 and AIF

Cornu ammonis segments and neuropile sections showing negative staining for caspase-3 in the pyramidal neurons, and neurons of the rabies infected dog (A), cat (B), and control animals (C). Negative staining for AIF in the dentate gyrus cells or neuropile tissue of the rabies-infected dog (D), cat (E) and control (F) animals. Pyramidal neurons in the cornu ammonis showing strong positive signals for LC3B in the rabies-infected dog (G) and cat (H). (I) Control. IHC × 20

results, the lowest Ct value was 29.72 °C in the dogs and the highest was 30.88 °C in the horses.

Immunohistochemistry results

The caspase-3, AIF, and LC3B expressions were investigated in the cerebellum and cornu ammonis sections of the naturally rabies-infected different animal species. The caspase-3 and AIF immunopositive cells were undetected in the cerebellum sections of the control (Figure 1D, H, L) and the cows (Figure 1A, E), horses (Figure 1B, F), and donkeys (Figure 1C, G). In contrast, as shown in Figure 1I–K, the LC3B immunopositivity was intensely observed in the cerebellum sections of the different animal species and was found in the cytoplasm of the Purkinje cells in the cer-
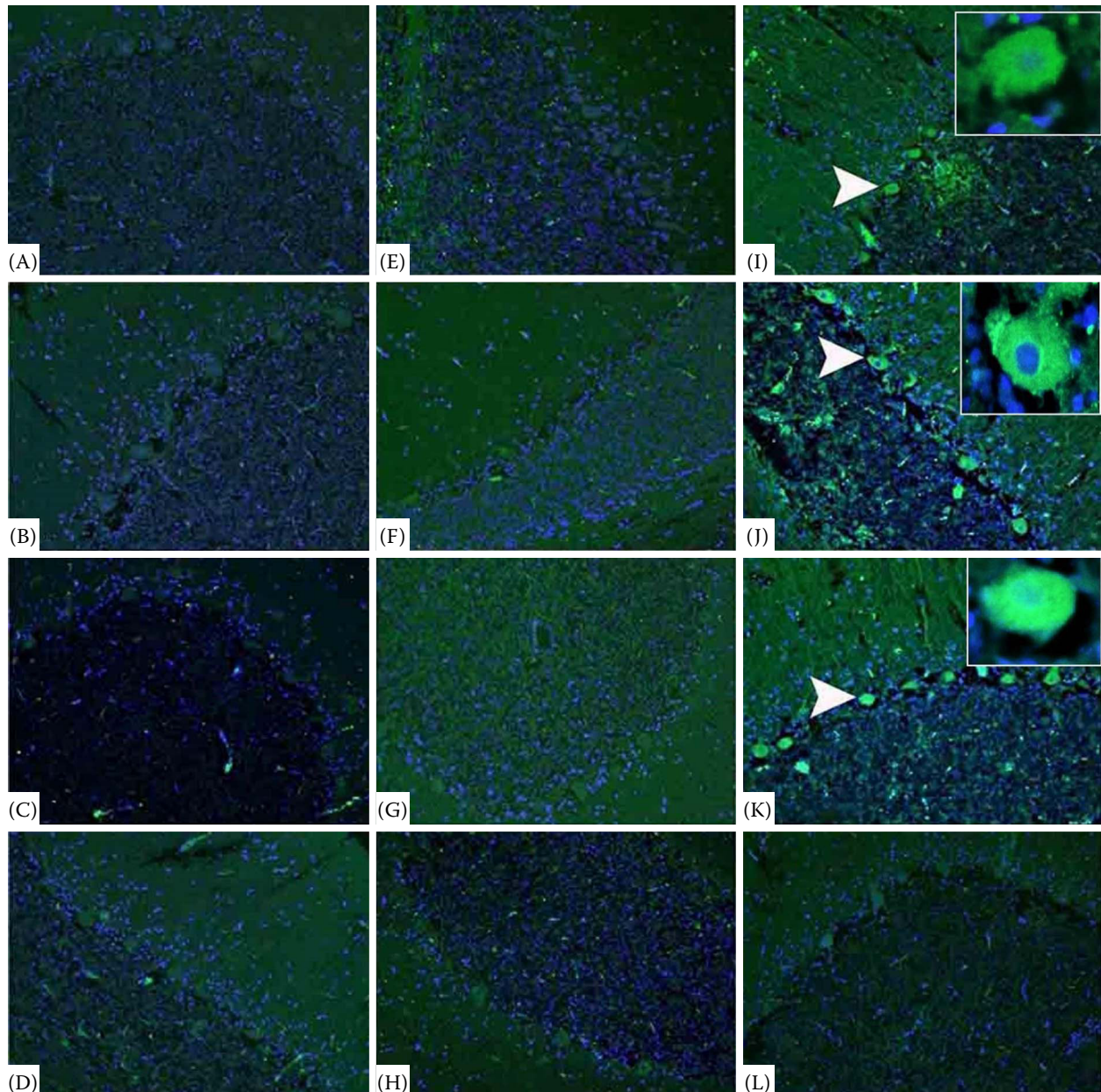
Figure 3. Representative fluorescence micrographs showing the positivity and negativity of caspase-3, AIF, and LC3B in the cerebellum of the rabies-infected animals by immunofluorescence

Control group (D, H, L) shows negative caspase-3, AIF, and LC3B immunoreactivity. Most of the granule cells and Purkinje cell compartments in the cerebellum of the rabies-infected cow (A), horse (B), and donkey (C) animals were caspase-3 negative. View of the negative AIF immunostaining reaction in the granule cells and Purkinje cell compartments in the cerebellum of the rabies-infected cow (E), horse (F), and donkey (G). Purkinje cell compartments of the cerebellum showing strong and diffuse LC3B positive signals with bright green fluorescence in the rabies-infected cow (I), horse (J), and donkey (K). FITC × 20

ebellum. Similarly, in the cornu ammonis of the control (Figure 2C, F, I) and the rabies-infected dogs (Figure 2A, D) and cats (Figure 2B, E), immunopositivity for caspase-3 and AIF was not detected, whereas these infected animals intensely exhibited LC3B immunopositivity (Figure 2G, H).

Immunofluorescence results

To determine whether the immunohistochemical data were correctly showing for the caspase-3, AIF, and LC3B positivity and negativity, immunofluorescence staining was performed. The results
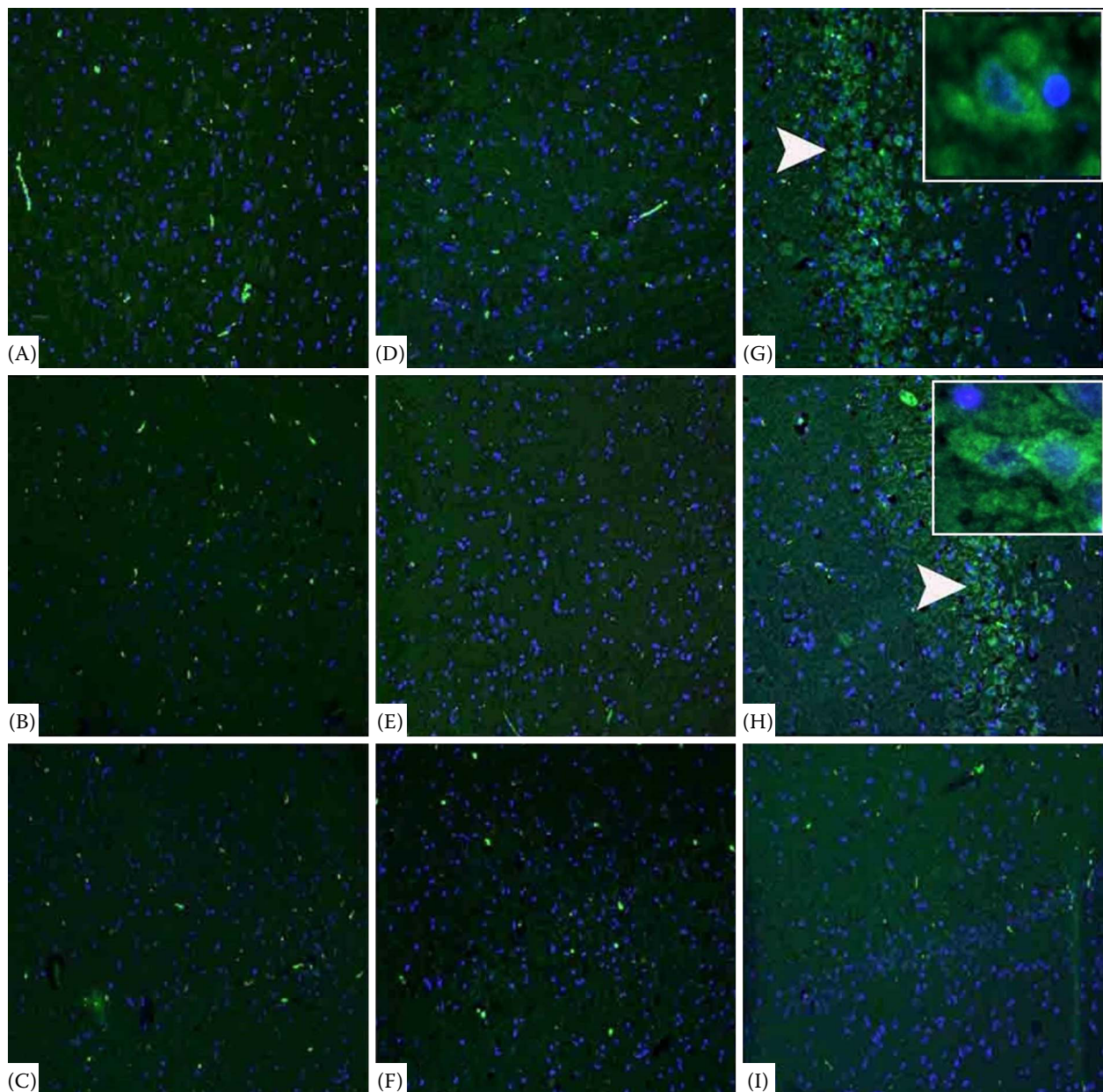
Figure 4. Representative fluorescence micrographs showing the positivity and negativity of caspase-3, AIF, and LC3B in the cornu ammonis segments and neuropile sections of the rabies-infected animals by immunofluorescence

Control group (C, F, I) shows negative caspase-3, AIF, and LC3B immunoreactivity. Neurons in the neuropile tissue of the rabies-infected dog (A) and cat (B) animals were caspase-3 negative. View of the negative AIF immunostaining reaction in the neurons in the neuropile tissue of the rabies-infected dog (D) and cat (E). Pyramidal neurons in cornu ammonis showing strong LC3B-positive signals with bright green fluorescence in the rabies-infected dog (G) and cat (H). FITC × 20

of the immunofluorescence staining showed that there was no marked difference in the caspase-3, AIF, and LC3B immunopositivity according to the immunohistochemistry results. The caspase-3 and AIF immunopositivity did not show an individual difference in the control (Figure 3D, H, L, and Figure 4C, F, I) and the rabies-infected cows (Figure 3A, E), horses (Figure 3B, F), donkeys (Figure 3C, G), dogs (Figure 4A, D), and cats (Figure 4B, E). However, the LC3B immunopositivity was compatible with the immunohistochemistry results. Namely, LC3B showed intense positivity both in the cerebellum sections of the rabies-infected cows (Figure 3I), donkeys (Figure 3J), and horses (Figure 3K) and in the cornu ammonis sections of the dogs (Figure 4G) and cats (Figure 4H).
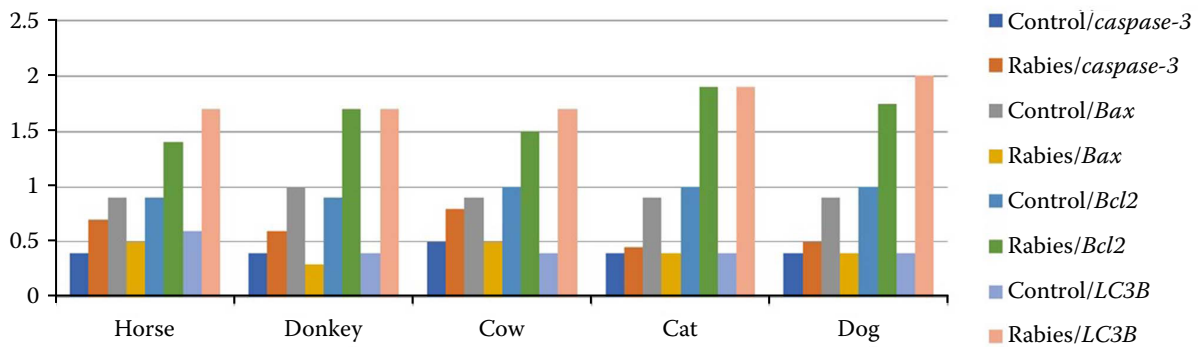
Figure 5. mRNA transcript levels of the *caspase-3*, *Bax*, *Bcl2* and *LC3B* genes in the brain tissues

Values represent the mean ± SE of three independent experiments for each sample. Statistical significance was analysed using a one-way ANOVA ($P < 0.001$)

Expression profiles of *caspase-3, Bax, Bcl2, and LC3B*

The expression levels of the *caspase-3*, *Bax*, *Bcl2* and *LC3B* genes in the rabies-positive cow, horse, donkey, dog and cat brain tissues were determined by qPCR. The *caspase-3* expression levels in the infected brain tissues were increased compared to the control group. However, this increase was not statistically significant ($P > 0.05$). When the *LC3B* expression level was examined, it was observed that *LC3B* was up-regulated to a statistically significant level in the rabies-positive brain tissues compared to the control groups ($P < 0.01$). In addition, it was observed that the expression of the *LC3B* gene in the dogs and cats was higher than that of the cows, horses and donkeys. Moreover, while the expression level of *Bax* was down-regulated in the infected brain tissues compared to control group ($P < 0.05$), the *Bcl2* expression level was up-regulated ($P < 0.05$) (Figure 5).

DISCUSSION

As a defence mechanism against viruses, apoptosis limits viral replication by eliminating the infected cells. However, this process also contributes to the spread of the virus (Zan et al. 2016). Various studies have been conducted to investigate apoptosis by use of cell cultures and using animals infected with different strains of the rabies virus (Jackson and Rossiter 1997; Jackson and Park 1998; Thoulouze et al. 2003; Sarmento et al. 2006; Scott et al. 2008). Autophagy, which is directly associated with the pathogenicity or replication of viruses, has been reported as a type of cell death that can take place before apoptosis

in viral infections (Alexander et al. 2007; Maiuri et al. 2007; Rodriguez-Rocha et al. 2011; Tang et al. 2013; Sharma et al. 2014). This study investigated the efficacy of the autophagic cell death model in addition to the apoptotic cell death in different animal species with a natural rabies infection.

In the initial studies conducted on the subject, it was reported that the virus caused apoptosis in suckling and adult mice (Jackson and Rossiter 1997; Jackson and Park 1998). In subsequent studies on rabies in humans, it was found that apoptosis did not play an important role (Rossiter and Jackson 2007; Fernandes et al. 2011). In contrast to caspase-dependent apoptosis in which caspases are present in apoptosis, caspase-independent apoptosis involving proteases, such as cathepsins, calpain or AIF, has been observed (Susin et al. 1999; Daugas et al. 2000; Galluzzi et al. 2012). Both cell culture and experimental studies performed in mice have produced different results, though different virus strains were used in these studies (Yan et al. 2001; Sarmento et al. 2005; Sarmento et al. 2006; Scott et al. 2008; Suja et al. 2011; Zan et al. 2016).

In cell culture studies, the virus has been reported to induce caspase-dependent and AIF-containing caspase-independent apoptosis (Thoulouze et al. 2003). While the challenge virus has been shown to cause caspase-dependent and AIF-mediated caspase-independent apoptosis in the cell culture, this type of apoptosis was not reported in a study on the silver-haired bat (Sarmento et al. 2006; Zan et al. 2016). In experimental studies conducted in mice [and in addition to the silver-haired bat rabies virus (SHBRV)] (Yan et al. 2001; Sarmento et al. 2005), it has been determined that street viruses (SV9) do not cause apoptosis (Suja et al. 2011). However, in another study that used the challenge virus

standard (CVS), apoptotic cell death was found to be very rare in the neurons (Scott et al. 2008).

This study is the first investigation of its kind to use gene expression, immunohistochemistry and immunofluorescence methods to demonstrate that no caspase-dependent (caspase-3) apoptosis occurs in cases of lethal rabies infections in animals. In addition, it has been shown, for the first time, that there is no involvement of AIF-containing caspase (as evaluated by the immunohistochemistry and immunofluorescence methods). The reason why apoptosis was detected in previous *in vivo* and *in vitro* studies and not in this investigation is probably due to the strains, pathogenicity, or viral activation of the autophagic cell death without activating the apoptotic cell death in animals with a natural infection.

Autophagy, which is currently the subject of much research, is a condition which protects cells under oxidative stress (Czaja 2011; Yap et al. 2016). In the case of autophagy encoded by autophagy-related genes, LC3B is a commonly used marker to demonstrate autophagy (Kirkegaard et al. 2004; Yang et al. 2005; Xie and Klionsky 2007; Klionsky et al. 2012). Studies conducted on the relationship between the rabies virus and autophagy are scarce. In *in vitro* studies, it was shown that the virus caused autophagy (LC3B) with increased LC3B levels (Peng et al. 2016; Li et al. 2017; Liu et al. 2017). Our study is the first report of LC3B-mediated autophagy in animals that died of a natural rabies infection as detected by the gene expression, immunohistochemistry, and immunofluorescence methods.

In conclusion, this study investigated the effectiveness of apoptosis and autophagy in rabies-infected cows, horses, donkeys, dogs, and cats. It has been observed that the expression level and immunopositive of LC3B in brain tissues infected with rabies is much higher than that of caspase-3. The experimental results provided by the different methods are in agreement with respect to the overall conclusions. Furthermore, it has been identified, for the first time, that the virus caused neuronal death in the central nervous system by autophagy, not by caspase-dependent (caspase-3) and AIF-containing caspase-independent apoptosis.

Conflict of interest

The authors declare no conflict of interest.

REFERENCES

Adams JM, Cory S. The Bcl-2 protein family: Arbiters of cell survival. Science. 1998 Aug;281(5381):1322-6.

Alexander DE, Ward SL, Mizushima N, Levine B, Leib DA. Analysis of the role of autophagy in replication of herpes simplex virus in cell culture. J Virol. 2007;81(22):12128-34.

Ashkenazi A, Dixit VM. Death receptors: Signaling and modulation. Science. 1998 Aug;281(5381):1305-8.

Budihardjo I, Oliver H, Lutter M, Luo X, Wang X. Biochemical pathways of caspase activation during apoptosis. Annu Rev Cell Dev Biol. 1999 Nov;15:269-90.

Comakli S, Ozdemir S, Degirmencay S. Canine distemper virus induces downregulation of $GABA_A$, $GABA_B$, and GAT1 expression in brain tissue of dogs. Arch Virol. 2020 Apr;165(6):1321-31.

Czaja MJ. Two types of autophagy are better than one during hepatocyte oxidative stress. Autophagy. 2011 Jan;7(1):96-7.

Daugas E, Nochy D, Ravagnan L, Loeffler M, Susin SA, Zamzami N, Kroemer G. Apoptosis-inducing factor (AIF): A ubiquitous mitochondrial oxidoreductase involved in apoptosis. FEBS Lett. 2000 Jul 7;476(3):118-23.

Dumrongphol H, Srikiatkhachorn A, Hemachudha T, Kotchabhakdi N, Govitrapong P. Alteration of muscarinic acetylcholine receptors in rabies viral-infected dog brains. J Neurol Sci. 1996 Apr;137(1):1-6.

Fernandes ER, de Andrade HF Jr, Lancellotti CL, Quaresma JA, Demachki S, da Costa Vasconcelos PF, Duarte MI. In situ apoptosis of adaptive immune cells and the cellular escape of rabies virus in CNS from patients with human rabies transmitted by Desmodus rotundus. Virus Res. 2011 Mar;156(1-2):121-6.

Galluzzi L, Kepp O, Trojel-Hansen C, Kroemer G. Mitochondrial control of cellular life, stress, and death. Circ Res. 2012 Oct 12;111(9):1198-207.

Giotakis AI, Kontos CK, Manolopoulos LD, Sismanis A, Konstadoulakis MM, Scorilas A. High BAX/BCL2 mRNA ratio predicts favorable prognosis in laryngeal squamous cell carcinoma, particularly in patients with negative lymph nodes at the time of diagnosis. Clin Biochem. 2016 Aug;49(12):890-6.

Granville DJ, Gottlieb RA. Mitochondria: Regulators of cell death and survival. ScientificWorldJournal. 2002 Jun 11; 2:1569-78.

Huang F, Huang M, Zhang H, Zhang C, Zhang D, Zhou G. Changes in apoptotic factors and caspase activation pathways during the postmortem aging of beef muscle. Food Chem. 2016 Jan 1;190:110-4.

Jackson AC, Park H. Apoptotic cell death in experimental rabies in suckling mice. Acta Neuropathol. 1998 Feb;95(2): 159-64.

Jackson AC, Rossiter JP. Apoptosis plays an important role in experimental rabies virus infection. J Virol. 1997 Jul;71(7):5603-7.

Jackson AC. Cholinergic system in experimental rabies in mice. Acta Virol. 1993 Dec;37(6):502-8.

Jackson AC. Rabies virus infection: An update. J Neurovirol. 2003 Apr;9(2):253-8.

Jackson AC. Therapy of human rabies. Adv Virus Res. 2011;79:365-75.

Kip E, Naze F, Suin V, Vanden Berghe T, Francart A, Lamoral S, Vandenabeele P, Beyaert R, Van Gucht S, Kalai M. Impact of caspase-1/11, -3, -7, or IL-1β/IL-18 deficiency on rabies virus-induced macrophage cell death and onset of disease. Cell Death Discov. 2017 Mar 6;3:17012.

Kirkegaard K, Taylor MP, Jackson WT. Cellular autophagy: Surrender, avoidance and subversion by microorganisms. Nat Rev Microbiol. 2004 Apr;2(4):301-14.

Klionsky DJ, Abdalla FC, Abeliovich H, Abraham RT, Acevedo-Arozena A, Adeli K, Agholme L, Agnello M, Agostinis P, Aguirre-Ghiso JA et al. Guidelines for the use and interpretation of assays for monitoring autophagy. Autophagy. 2012 Apr;8(4):445-544.

Li L, Jin H, Wang H, Cao Z, Feng N, Wang J, Zhao Y, Zheng X, Hou P, Li N, Chi H, Huang P, Jiao C, Li Q, Wang L, Wang T, Sun W, Gao Y, Tu C, Hu G, Yang S, Xia X. Autophagy is highly targeted among host comparative proteomes during infection with different virulent RABV strains. Oncotarget. 2017 Mar 28;8(13):21336-50.

Liu J, Wang H, Gu J, Deng T, Yuan Z, Hu B, Xu Y, Yan Y, Zan J, Liao M, DiCaprio E, Li J, Su S, Zhou J. BECN1-dependent CASP2 incomplete autophagy induction by binding to rabies virus phosphoprotein. Autophagy. 2017 Apr 3;13(4):739-53.

Livak KJ, Schmittgen TD. Analysis of relative gene expression data using real-time quantitative PCR and the $2^{-\Delta\Delta CT}$ method. Methods. 2001 Dec;25(4):402-8.

Maiuri MC, Zalckvar E, Kimchi A, Kroemer G. Self-eating and self-killing: Crosstalk between autophagy and apoptosis. Nat Rev Mol Cell Biol. 2007 Sep;8(9):741-52.

Nagaraj T, Vasanth JP, Desai A, Kamat A, Madhusudana SN, Ravi V. Ante mortem diagnosis of human rabies using saliva samples: Comparison of real time and conventional RT-PCR techniques. J Clin Virol. 2006 May;36(1):17-23.

Nan L, Xie Q, Chen Z, Zhang Y, Chen Y, Li H, Lai W, Chen Y, Huang M. Involvement of PARP-1/AIF signaling pathway in protective effects of Gualou Guizhi decoction against ischemia-reperfusion injury-induced apoptosis. Neurochem Res. 2020 Feb;45(2):278-94.

Peng J, Zhu S, Hu L, Ye P, Wang Y, Tian Q, Mei M, Chen H, Guo X. Wild-type rabies virus induces autophagy in human and mouse neuroblastoma cell lines. Autophagy. 2016 Oct 2;12(10):1704-20.

Rodriguez-Rocha H, Gomez-Gutierrez JG, Garcia-Garcia A, Rao XM, Chen L, McMasters KM, Zhou HS. Adenoviruses induce autophagy to promote virus replication and oncolysis. Virology. 2011 Jul 20;416(1-2):9-15.

Rossiter JP, Jackson AC. Pathology. In: Jackson AC, Wunner WH, editors. Rabies. London: Elsevier Academic Press; 2007. p. 383-9.

Sarmento L, Li XQ, Howerth E, Jackson AC, Fu ZF. Glycoprotein-mediated induction of apoptosis limits the spread of attenuated rabies viruses in the central nervous system of mice. J Neurovirol. 2005 Dec;11(6):571-81.

Sarmento L, Tseggai T, Dhingra V, Fu ZF. Rabies virus-induced apoptosis involves caspase-dependent and caspase-independent pathways. Virus Res. 2006 Nov;121(2):144-51.

Scott CA, Rossiter JP, Andrew RD, Jackson AC. Structural abnormalities in neurons are sufficient to explain the clinical disease and fatal outcome of experimental rabies in yellow fluorescent protein-expressing transgenic mice. J Virol. 2008 Jan;82(1):513-21.

Sharma M, Bhattacharyya S, Nain M, Kaur M, Sood V, Gupta V, Khasa R, Abdin MZ, Vrati S, Kalia M. Japanese encephalitis virus replication is negatively regulated by autophagy and occurs on LC3-I- and EDEM1-containing membranes. Autophagy. 2014 Sep;10(9):1637-51.

Shinoura N, Yoshida Y, Asai A, Kirino T, Hamada H. Relative level of expression of Bax and Bcl-XL determines the cellular fate of apoptosis/necrosis induced by the overexpression of Bax. Oncogene. 1999 Oct 7;18(41):5703-13.

Suja MS, Mahadevan A, Madhusudana SN, Shankar SK. Role of apoptosis in rabies viral encephalitis: A comparative study in mice, canine, and human brain with a review of literature. Patholog Res Int. 2011;2011:374286.

Susin SA, Lorenzo HK, Zamzami N, Marzo I, Snow BE, Brothers GM, Mangion J, Jacotot E, Costantini P, Loeffler M, Larochette N, Goodlett DR, Aebersold R, Siderovski DP, Penninger JM, Kroemer G. Molecular characterization of mitochondrial apoptosis-inducing factor. Nature. 1999 Feb 4;397(6718):441-6.

Tang SW, Chen CY, Klase Z, Zane L, Jeang KT. The cellular autophagy pathway modulates human T-cell leukemia virus type 1 replication. J Virol. 2013 Feb;87(3):1699-707.

Thoulouze MI, Lafage M, Yuste VJ, Baloul L, Edelman L, Kroemer G, Israel N, Susin SA, Thoulouze MI, Lafage M, Yuste VJ, Baloul L, Edelman L, Kroemer G, Israel N, Susin SA, Lafon M. High level of Bcl-2 counteracts apoptosis mediated by a live rabies virus vaccine strain and induces long-term infection. Virology. 2003 Sep 30;314(2):549-61.

Vahed SZ, Barzegari A, Rahbar Saadat Y, Mohammadi S, Samadi N. A microRNA isolation method from clinical samples. Bioimpacts. 2016;6(1):25-31.

Warrell MJ, Warrell DA. Rabies and other lyssavirus diseases. Lancet. 2004 Mar 20;363(9413):959-69.

Xie Z, Klionsky DJ. Autophagosome formation: Core machinery and adaptations. Nat Cell Biol. 2007 Oct;9(10):1102-9.

Yan X, Prosniak M, Curtis MT, Weiss ML, Faber M, Dietzschold B, Fu ZF. Silver-haired bat rabies virus variant does not induce apoptosis in the brain of experimentally infected mice. J Neurovirol. 2001 Dec;7(6):518-27.

Yang YP, Liang ZQ, Gu ZL, Qin ZH. Molecular mechanism and regulation of autophagy. Acta Pharmacol Sin. 2005 Dec;26(12):1421-34.

Yap YW, Llanos RM, La Fontaine S, Cater MA, Beart PM, Cheung NS. Comparative microarray analysis identifies commonalities in neuronal injury: Evidence for oxidative stress, dysfunction of calcium signalling, and inhibition of autophagy-lysosomal pathway. Neurochem Res. 2016 Mar;41(3):554-67.

Youle RJ, Strasser A. The BCL-2 protein family: Opposing activities that mediate cell death. Nat Rev Mol Cell Biol. 2008 Jan;9(1):47-59.

Zan J, Liu J, Zhou JW, Wang HL, Mo KK, Yan Y, Xu YB, Liao M, Su S, Hu RL, Zhou JY. Rabies virus matrix protein induces apoptosis by targeting mitochondria. Exp Cell Res. 2016 Sep 10;347(1):83-94.